Proceedings of 7th ICFDP7
Seventh International Congress on Fluid Dynamics & Propulsion
December 18-20, 2001,Cairo, Egypt

ICFDP7-2001020

PREDICTION OF ENGINE INTAKE FILTER PERFORMANCE AND ITS IMPACT ON ENGINE EROSION IN CAIRO CITY

Ahmed F. Abdel Azim
Professor of Fluid Mechanics, Zagazig University

Hafez A. El-Salmawy
Associate Professor, Zagazig University

Mohamed M. Shamloul
Associate Professor, Zagzig University

Osama M. Mesalhy
Teaching Assistant, Zagazig University

ABSTRACT

Numerical solution has been developed for the performance of the engine intake filter. The developed solution predicts the dust particle size distribution as well as the particles loading ratio downstream the filter. Also the solution provides the evolution of the filter performance over its lifetime. The developed solution has been integrated with a previously developed engine model to predict erosion in the engine internal surfaces due to the ingested dust particles. A case study for erosion in engine cylinders in Cairo city has been carried out using the developed filter solution as well as the engine erosion model. This case study relies on measured values for particle size distribution of suspended dust at some areas in Cairo. The results showed that the cellulose filter has a substantial effect on both particle size and loading ratio ingested into the engine during the intake process. The reduction in engine erosion due to the use of intake filter is varied among the different engine parts. Erosion is reduced by 92.5 %, 98.1 %, and 97.9 % for the cylinder head, inlet valve face and piston face respectively. Also oil contamination with particles is reduced by 98.2 %. On the other hand the loss in engine output does not exceed 2% by the end of the filter lifetime.

INTRODUCTION

Dirt is the main cause of metal wear in engines. According to Fodor [1,2] about 80% of all engine failures are attributed to engine wear. Elkotb [3] pointed out that 60% of the failures of the new engines in the public transportation buses in Cairo is attributed to the dust particles entering into the engine cylinders. Engine wear is attributed to both direct and indirect effect of the ingested particles. The direct effect comes from the dust particles as they impact the engine internal surfaces during different engine processes, especially the inlet and exhaust valves as well as their seats [4]. Also it is attributed to the slip of the dust particles into piston crevices. The indirect effect is attributed to the fact that substantial part of particles ingested into the engine during the intake process ends up in the lubricating oil. This degrades the oil quality and consequently increases engine wear. Therefore induction air filter is an essential element to protect the engine from wear and improve its durability.

The ambient dust concentrations can vary from 0.1 mg/m^3 to 1000 mg/m^3 depending on the environmental and the driving conditions [5]. It has been found that the air cleanliness ingested by the engine should be less than 0.01 mg/m^3 to reduce wear [6]. The ambient dust concentration levels have been divided into three ranges:

1. Normal driving conditions (0.1-1.0 mg/m^3) like; rural highways, urban highways, country roads, residential areas, etc.. In order to meet the downstream criteria of 0.01 mg/m^3, it is required for the engine air filter to have a collection efficiency in the rage of 95 % to 99.0%.
2. Dusty conditions (0.5-50 mg/m^3) like ; congested urban highways, congested city roads, industrial areas, unpaved roads, etc.. The required efficiency of the filter should be in the range between 99% and 99.98%.
3. Very dusty conditions (10-1000 mg/m^3) like; dust storms, mining operations, agricultural areas, etc.. The required efficiency should be in the range of 99.8% to 99.999%.

As it is very important to remove or control the dust concentrations being ingested into the engine, it is also critical

to control the dust particles sizes most harmful to the engine. Maximum wear is caused by the particles having size range of 5-15 μm [4]. On the other hand, dirt and abrasive particles diameters equal to or less than the oil film thickness separating various sliding and rotating parts cause excessive wear. Even fine particles (<1μm) may cause excessive wear, if their concentration is high enough to agglomerate [7].

Wai and Lui [8] studied experimentally the performance of a cellulose and foam filter media for engine air cleaning applications. Their study covered both phenolic and non-phenolic cellulose filters. Flat-sheet and pleated cellulose filters were also included in this study. Both filter pressure drop and fractional collection efficiency had been measured in the experiments as a function of the particle size. The fractional collection efficiency equals to the ratio between the mass collected by the filter to the total particle mass entered the filter. Laser based particle analyzer has been used to measure both particle sizes and concentrations before and after the filter. According to these measurements, it has been found that, pressure drop across the filter increases with the increase in the dust loading. This is attributed to the clogging of the flow paths as more dust is collected. On the other hand, a dust cake in formed on the filter surface. It acts as a very efficient filter. This cake adds to the pressure drop across the filter. The characteristic relations for the pressure drop at different mass loading for different types of filter materials considered in Wai and Lui experiments, is shown in Fig. 1. This curve can be interpreted in a way that it represents the change in the filter pressure drop over the filter life time. Regarding the characteristic relation between the different particles sizes and the collection efficiency, Fig.2 shows such relation for a cellulose filter at different accumulated mass of the dust inside the filter.

Although these measurements are quite informative however they do not offer comprehensive information for dust conditions downstream the filter. This information should include the particle size distribution and mass loading ratio based on the particle size distribution and the mass loading upstream the filter. Furthermore the change in these quantities over the filter lifetime is needed. This information are necessary to predict erosion in the engine internal surfaces, where both the particle size and loading ratio have effects on the intensity as well as the location of the eroded surfaces inside the engine [4].

This paper aims at predicting the particle size distribution as well as the loading ratio of the dust particles downstream the intake filter. It will consider evolution of filter performance with time. The technique adopted is partially

Error! Not a valid link.

Fig.1 Pressure Drop Across a Cellulose Filter as a Function in Mass Loading [8]

Error! Not a valid link.

Fig.2 Collection Efficiency of Filter at Different Particle Sizes [8]

imental and partially numerical. It relies on the urements of the characteristic relation between the particle and the fractional collection efficiency at different itions of accumulated dust in the filter. The measurements e characteristic relation between the mass loading and the pressure drop across the filter will be considered too. These two aforementioned characteristic relations are numerically discritized and manipulated such that it became possible to calculate the particle loading ratio, particle size and mass fraction for each partic lefined input data for particle size distribution and loading ratio. The produced results will be used as an input data to the previously developed engine model to calculate the intensity as well as location of erosion inside the engine [4]. Since the prediction is a function in the input particle size distribution and its loading ratio a case study, which relies on measurements for particle size distribution at different areas in Cairo city is considered. Accordingly, the developed solution presents a prediction for erosion in the engines working in Cairo city.

NOMENCLATURE

d	:	Particle diameter (μm)
m	:	mass (mg)
q	:	Rosen Ramller Expression Constant
Q^o	:	Engine Flow rate (m^3/sec)
δm	:	Mass Change (mg)
t	:	Time (sec)
u	:	Velocity (m/s)
Y_{rt}	:	Yield strength at room temperature
Y_s	:	Yield strength at temperature T
ρ	:	Density (kg/m^3)
η_c	:	Collection Efficiency (%)
φ	:	Loading ratio (mg/m^3)

Subscripts

AF	:	After the Filter
av	:	Average
BF	:	Before the Filter
i	:	interval
T	:	Total

INTAKE FILTER MODEL

The pressure drop across the filter is a function in the mass of dust accumulated inside the filer, as shown in Fig.1. On the other hand, the characteristic relation of the fractional collection efficiency at each particle size depends on the

accumulated mass inside the filter, as shown in Fig.2. For simplicity, the filter service life will be divided into three intervals. These intervals are: new, intermediate and end life. Each interval is defined as the interval at which the accumulated mass inside the filter increased by one third of the total mass at which the filter service life is expired. The service life of the filter is expired when the pressure drop across the filter reaches a threshold value of 1500 Pa. [8]. Accordingly, the characteristic relation shown in Fig.1 for a filter having a cellulose media has been divided into three equal intervals, as shown in Fig.3. The pressure drop across each interval has been averaged. It is important to point out that, both the collection efficiency and consequently the pressure drop across the filter depend on the face mass velocity. The pressure drop increases with the increase in this velocity. This relation represents a characteristic relation of the filter media. However, the face velocity depends on the engine air flow rate and the surface area of the filter. Therefore it represents a design criterion. This value has been taken as 12.7 cm/s for the used filter material. Accordingly the three averaged values of the pressure drop over the filer service life will be taken as boundary conditions. The switch from each life phase to another depends on the accumulated mass inside the filter.

Error! Not a valid link.

Fig.3 Intervals of Mass Loading Versus the Pressure Drop Across the Filter Along the Filter Lifetime

Fractional penetration, presented in Fig.2, has been tabulated as a function of the accumulated mass inside the filter for different particle diameters. For any intermediate value linear interpolation is used. Regarding the particle size distribution it is considered as Rosin Rammler distribution [9]. This distribution takes the following expression:

$$\frac{m}{m_T} = 1 - Exp - (\frac{d_p}{d'})^q \qquad (1)$$

Where d` and q are constants. The constant d' is the particle diameter such that 63.2% of the total particles mass is of smaller diameters. The exponent q provides a measure of the spread of the particle sizes. This distribution can be descritized into n diameter intervals as shown in Fig.4. According to each particle size class and filter service life interval, the particle loading ratio after the filter can be calculated as a function of the particle loading ratio before the filter. This can be done according to the following equation:

$$\Phi_{AF} = \sum_{i=1}^{i=n} \left(Exp-(\frac{d_{i-1}}{d'})^q - Exp-(\frac{d_i}{d'})^q \right) (1-\eta_c(d_{iav})) * \Phi_{BF} \qquad (2)$$

Where $d_{iav} = (d_{i-1}+d_i)/2$, d_0 and d_n are the minimum and maximum particle diameters of the particle size distribution respectively. Considering the loading ratio after the filter, the mass accumulated inside the filter can be calculated as follows:

$$\delta m = (\Phi_{BF} - \Phi_{AF}) \int_{\tau_o}^{\tau} Q^o * d\tau \qquad (3)$$

Error! Not a valid link. Fig. 4 Discritized Particle Size Distribution

If the accumulated mass inside the filter exceeded 1/3 or 2/3 of the total mass at which the filter lifetime is expired according to Fig.3, the pressure drop across the filter will be updated accordingly. Regarding the particle size distribution after the filter its mass fraction at each diameter d_{iav} can be calculated as follows:

$$\left(\frac{m}{m_T}\right)_{d_{iav}} = \frac{\left(Exp-(\frac{d_{i-1}}{d'})^q - Exp-(\frac{d_i}{d'})^q \right)(1-\eta_c(d_{iav}))}{\sum_{i=1}^{i=n}\left[\left(Exp-(\frac{d_{i-1}}{d'})^q - Exp-(\frac{d_i}{d'})^q \right)(1-\eta_c(d_{iav})) \right]} \qquad (4)$$

Accordingly all the input boundary values such as the inlet pressure, particles loading, particle size distribution necessary to calculate erosion are defined for each stage of filter lifetime. The engine erosion model previously developed [4] to predict erosion in the engine internal surfaces due to the ingested particles requests these boundary values. For the sake of completeness the model equations will be illustrated. More details can be found in ref. [4].

ENGINE CYLINDER EROSION MODEL

The engine erosion mathematical model consists of the governing equations for the reactive flow inside the engine cylinder, the particles trajectories, particles surface interaction and the surfaces erosion due the impact of the particles. These equations are as follows:

Continuity

$$\frac{\partial \rho_m}{\partial t} + \nabla.(\rho_m \vec{u}) = \nabla.\left[\rho D \nabla\left(\frac{\rho_m}{\rho} \right) \right] + S^c \qquad (5)$$

S^c is combustion source term

Momentum

$$\frac{\partial \rho \vec{u}}{\partial t} + \nabla.(\rho \vec{u}\vec{u}) = -\frac{1}{a^2}\nabla P - \nabla(\frac{2}{3}\rho k) + \nabla.\tau + F^s + \rho g \quad (6)$$

F^S is particle source term, which takes the following expression:

$$F^S = -\int F \rho_p (\frac{4}{3}\pi r_p^3 \frac{d\vec{u}_p}{dt}) d\vec{u} dr_p dt \quad (7)$$

Energy

$$\frac{\partial \rho I}{\partial t} + \nabla.(\rho \vec{u} I) = -P\nabla.\vec{u} - \nabla.J + \rho\varepsilon + Q^c + Q^s \quad (8)$$

J is the heat flux, which combines both heat conduction and enthalpy diffusion and Q^s is the source term due to particles presence, both can be expressed as follows:

$$J = -k\nabla T - \rho D \sum_m h_m \nabla\left(\frac{\rho_m}{\rho}\right) \quad (9)$$

$$Q^s = -\int F \rho_p \frac{4}{3}\pi r_p^3 \begin{bmatrix} Cp T_p + \\ F_d.(\vec{u}_p - \vec{u} - u') \end{bmatrix} d\vec{u}_p dr_p dT \quad (10)$$

Both S^c and Q^c in are source terms account for combustion. Their values are defined using a partial equilibrium model proposed in KIVA II code [10]. In this model the fast reactions are modeled as equilibrium reactions, while the slow reactions are modeled as rate reactions, which proceed kinetically.

Turbulent Kinetic Energy

$$\frac{\partial \rho k}{\partial t} + \nabla.(\rho \vec{u} k) = -\frac{2}{3}\rho k \nabla.\vec{u} + \tau : \nabla\vec{u} + \nabla.\left[\left(\frac{\mu}{\mathrm{Pr}_k}\right)\nabla k\right] - \rho\varepsilon + W^S \quad (11)$$

Where

$$W^S = -\int F \rho_p \left(\frac{4}{3}\pi r_p^3 \frac{d\vec{u}_p}{dt}.\vec{u}_p\right) d\vec{u}_p dr_p dt \quad (12)$$

Dissipation of Turbulent Kinetic Energy

$$\frac{\partial \rho \varepsilon}{dt} + \nabla.(\rho \vec{u} \varepsilon) = -\left(\frac{2}{3}C_{\varepsilon 1} - C_{\varepsilon 3}\right)\rho\varepsilon\nabla.\vec{u} + \nabla.\left[\left(\frac{\mu}{P_{r\varepsilon}}\right)\nabla\varepsilon\right] + \frac{\varepsilon}{k}\left[C_{\varepsilon 1}\tau : \nabla\vec{u} - C_{\varepsilon 2}\rho\varepsilon + C_S W^S\right] \quad (13)$$

The constants $C_{\varepsilon 1}$, $C_{\varepsilon 2}$, $C_{\varepsilon 3}$, P_{rk}, $P_{r\varepsilon}$ and C_S have the values 1.44, 1.92, -1.0, 1.0, 1.3 and 1.5 respectively.

Turbulence generation due to the presence of the particles is expressed by adopting a pseudo viscosity term, which is added to the turbulent viscosity. The following relation gives this term:

$$\mu_S = Const.*\varphi_p \rho r_p \left|\vec{u} - \vec{u}_p\right| \quad (14)$$

On the other hand W^S presented in equation (12) expresses turbulence destruction, due to the presence of the particles. As shown W^S has a negative value.

Particle Momentum

$$\frac{d\vec{u}_p}{dt} = \frac{3\rho}{8\rho_p}\frac{\left|\vec{u} + \vec{u}' - \vec{u}_p\right|}{r_p}\left(\vec{u} + \vec{u}' - \vec{u}_p\right)C_D \quad (15)$$

Drag coefficient C_D is given by the following relation:

$$C_D = \begin{cases} \frac{24}{\mathrm{Re}}\left(1 + (1/6)\,\mathrm{Re}^{3/2}\right) & \mathrm{Re} < 1000 \\ 0.424 & \mathrm{Re} > 1000 \end{cases} \quad (16)$$

Re is the Reynolds number which takes the following expression:

$$\mathrm{Re} = \frac{2\rho\left|\vec{u} + \vec{u}' - \vec{u}_p\right| r_p}{\mu_{air}} \quad (17)$$

The turbulent component ú is assumed to follow a Gaussian distribution with mean square deviation (2/3)k, thus:

$$G(\vec{u}') = (\frac{4}{3}\pi k)^{-3/2} Exp(-3\left|\vec{u}'\right|^2 / 4k) \quad (18)$$

Value of $\vec{u}'$ is chosen stochastically once every turbulence correlation time t_{turb} otherwise it is held constant. The turbulence correlation time is given by:

$$t_{turb} = \min(k/\varepsilon, cps\frac{k}{\varepsilon}\frac{1}{\left|\vec{u}+\vec{u}'-\vec{u}_p\right|}) \quad (19)$$

Where cps is an empirical constant with a value of 0.16432. Thus t_{turb} is the minimum of an eddy breakup time (k/ε) and time of particle to traverse an eddy.

Particle Surface Interaction

A stochastic model for particle rebound has been used. The Monte Carlo method is used to evaluate the random values of the rebound particles velocities and angles. The stochastic functions for both velocity and angle take the following form:

$$F(x) = \frac{1}{\sigma\sqrt{2\pi}}\int_{-\infty}^{(x-\mu)/\sigma} e^{-u^2/2}\sigma du = \Phi\left(\frac{x-\mu}{\sigma}\right) \quad (20)$$

Where Φ is a tabulated function and μ and σ are the mean and standard deviation respectively. Their values are obtained from the experiments carried out by Hamed [11]

Erosion Equations

The erosion model relies on the cutting and deformation model developed by Grant [12]. According to this model the erosion parameter has the following expression:

$$\varepsilon_r = K_1 f(\beta)\vec{u}_p^2 Cos^2\beta(1-R_\tau^2) + K_3(\vec{u}_p Sin\beta)^4 \quad (21)$$

Where:

$$R_\tau = 1.0 - 0.00525\vec{u}_p Sin\beta$$
$$f(\beta) = 1.0 + C_k(K_{12}Sin(\pi/2\beta/\beta_o))^2 \quad (22)$$

$$CK = \begin{cases} 1.0 & \beta \le 2\beta_o \\ 0.0 & \beta > 2\beta_o \end{cases} \quad (23)$$

The constants K_1, K_{12} and K_3 were taken for sand particles impacting steel and Aluminum alloys, as the piston and cylinder head are assumed to be Aluminum, while the cylinder wall and valves are assumed to be steel. The values of K_1, K_3 and K_{12} are 6.53E-8, 8.94E-13 gm/gm(m/s)^2 and 0.293 respectively for sand impacting steel surface, and 3.95E-8, 6.95E-13 gm/gm(m/s)^2 and 0.585 for sand impacting Aluminum surface.

The effect of temperature of the target surface is considered through multiplying the erosion parameter by a function of temperature F(T) as suggested by [13]. F(T) takes the following expression:

$$F(T) = \left[\left(\frac{Y_{rt}}{Y_s}\right)^{3.68} - \left(\frac{Y_s}{Y_{rt}}\right) + 1\right] \quad (24)$$

Numerical Solution

The developed model represents a modified version of KIVA II code [10]. The modifications include: addition of inlet and exhaust valves, introduction of solid particulates through the inlet valve using a stochastic scheme, consideration of full coupling between particles and flow including their effect on turbulence generation, modification of the wall heat transfer model to calculate the instantaneous wall temperature, addition of particle surface interaction model and inclusion of erosion model. Numerical solution followed is that used by KIVA II code. This solution relies on an arbitrary Lagrangian Eulerian scheme for the flow and Lagrangian scheme for the particles.

Boundary and Initial Conditions

The solution covers a full engine cycle starting from the piston at the TDC during the suction stroke. For the solid wall surfaces, the logarithmic law of wall was used for both velocity and temperature profiles. Regarding the inlet and the outlet boundaries they are set as continuative flow. Stagnation pressure and temperature are kept constant at atmospheric pressure and 300 ^{o}K respectively. The turbulent kinetic energy at the intake is assumed to be 10% of the mean flow kinetic energy at the boundary. The length scale is held constant and equals to half the maximum valve lift. It is import to mention that the particle size probability function at the intake is considered according to the developed filter model. The particles are introduced stochastically according to this size probability function.

The initial gas temperature and pressure are considered homogeneous and equal to 1.2 bar and 800 ^{o}K respectively. The residual gases composition is assumed as those corresponding to stoichiometric combustion gases of Octane. Initial cylinder turbulence is assumed homogeneous and equal to 10% of the energy of the mean piston speed kinetic energy. The initial length scale is set equal to half the clearance volume. Regarding the initial value for the dissipation of the turbulent kinetic energy, it can be determined from both the initial turbulent kinetic energy and length scale ($\varepsilon_{initial}=k^{3/2}$/initial length scale).

PARTICLE CONCENTRATIONS AND SIZE DISTRIBUTION IN CAIRO AIR

Regarding the size distribution of particles in Cairo air, the majority of the particles in Cairo air have diameters in the ranges of 4-8 μm [3]. Particles having larger sizes represent 5% in all regions except at Shobra Elkhima and Portland Tora, where larger particles represent 10-15% of the total particles distribution. The mean diameter in all regions is around 7μm.

The cumulative frequency curves of the particles size in different regions of Cairo are shown in Fig.6 [3]. Since these distributions are given in cumulative frequency (n/n_T), it is important first to convert them into cumulative mass fraction. This is be done according to the following equation:

$$\frac{m}{m_T})_{d_p} = \frac{\int_{d_{p_{min}}}^{d_p} (d_p)^3 d(\frac{n}{n_T})}{\int_{d_{p_{min}}}^{d_{p_{max}}} (d_p)^3 d(\frac{n}{n_T})} \qquad (25)$$

The resulted curve is fitted using Rosin Rammler expression, as stated in equation (1), and used as an input data to the filter solution.

RESULTS

The aforementioned solution has been applied for a case where the engine has the characteristics shown in Table 1. Filter with a cellulose media as well as surface velocity of 12.7 cm/sec are considered. Regarding the ambient particle size distribution and loading ratio those measured in Tora area were considered in this case study, as shown in Fig.6.

Considering the loading ratio of the suspended dust in Tora which is 19 mg/Nm^3 [3], the loading ratio down stream the filter during the different life intervals of the filter is predicted. Table 2 shows the ratio between the loading ratio down and up stream the filter for the different intervals of the filter lifetime.

ır! Not a valid link.

. (5) Cumulative Distribution of Particles in Different Regions in Cairo in City [3]

Table 1 Characteristics of the Engine

	Characteristic/ Value
ıe Type	Spark Ignition
	100 mm
e	120 mm
ecting Rod/Crank	2.71
l	1500 rpm
Compression Ratio	9
Spark Timing	20^o BTDC
Cooling Water Temp	
Valve Timing	
Intake Open	5^o BTDC
Intake Close	30^o ABDC
Exhaust Open	30^o BBDC
Exhaust Close	At TDC

Table 2 The Change in the Loading Ratio Down Steam The Filter Over Its lifetime.

Interval	First interval	Second interval	Third interval
Loading ratio downstream filter/ Loading ratio upstream filter	0.051	0.002	0.0015

According to Table (2) substantial reduction in the loading ratio is achieved as a result of using a cellulose filter. The impact of the filter on its downstream loading ratio increases along the filter service life. This is attributed to the improvement in the filter efficiency as a result of the formation of the dust cake on the filter surface as well as the narrowing of the filter internal passages as a result of dust accumulation.

Regarding the particle distribution down stream the filter during the first interval of the filter service life, Fig. 6 shows such distribution compared with the distribution upstream the filter. As shown from the Figure the filter impact is more pronounced for the large particles in comparison with the small one.

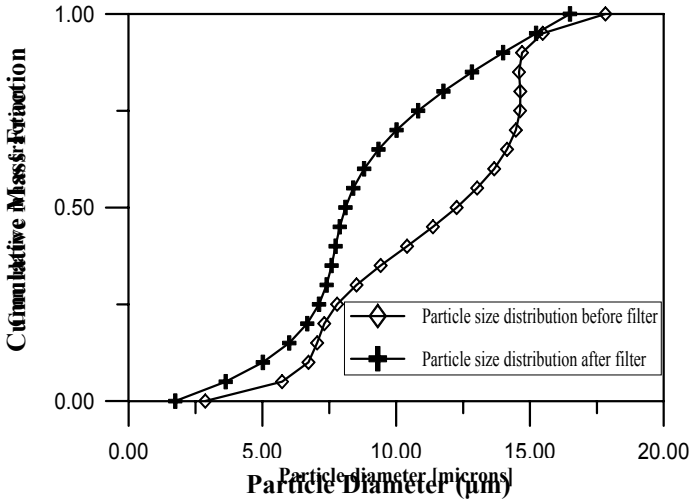

Fig. (6) Particle Size Distribution before and after Filtration.

Considering the pressure drop across the filter, the loading ratio and the particle distribution down stream the filter, the erosion in the different engine internal surfaces as well as oil particle contamination can be calculated, using the developed engine erosion model [4]. The particles are introduced to the engine stochastically according to the particle size distribution down stream the filter.

Table (3) shows the reduction in erosion in the engine internal surfaces due to the use of the intake filter in comparison with the condition where the filter is not used.

Also it shows the impact of using the filter on the rate of oil contamination as well as the reduction in the engine output power due to the impact of using an intake filter.

It is important to point out that according to Table (2) and (3) it can be noticed that erosion reduction in the cylinder head, which is the most critical part affected by particle erosion [4], is not consistent with the reduction in the loading ratio. This is attributed to the tendency of the filter to abate the large particles in favor of the small one. The small particles are more responsible for erosion in the cylinder head surface [4]. On the other hand, the erosion in the inlet valve and the piston faces, have closer values to the reduction in the loading ratio. The erosion in these parts is not sensitive to the change in the particle size distribution and it is mainly controlled by the loading ratio [4].

Table 3 Erosion in engine different parts, loss of engine power and oil contamination for different filter lifetime normalized by the corresponding values without filter

Case	Cyl. head	Valve face	Piston face	Power	Dust in Oil
1st interval	0.203	0.052	0.057	0.994	0.0488
2nd interval	0.008	0.002	0.002	0.9885	0.0019
3rd interval	0.008	0.001	0.002	0.9838	0.0014

As the total number of particles introduced to the engine due to the use of intake filter is reduced substationally, the percentage of particles that stuck on the cylinder surface and consequently go to the oil layer is reduced too.

Regarding the increase in the pressure drop across the filter over the filter lifetime, it is shown in Table (3) that, it has a minor effect on the engine power loss. This loss in power is around 1.62% by the end of the filter lifetime, which is equivalent to 1500 pa . On the other hand considering the mass accumulated inside the filter it is found that the filter service life time under Tora air quality is too short. This lifetime is 43 hour. It is important to mention that, filter lifetime can be increased by using larger size filter. This enables larger capacity of accumulated dust for the same pressure drop.

CONCLUSIONS

A Hybrid solution for the engine intake filter has been developed. This solution depends on experimental measurements as well as numerical manipulation. Comprehensive solution has been developed which provides detailed conditions as well as their evolution with time for the dust down stream the filter. These conditions include loading ratio, particle size distribution and inlet pressure, which are necessary boundary values for the erosion prediction model previously developed for the engine. The application of this solution showed that the engine intake filter has a substantial impact on the dust conditions ingesting into the engine. This led to a substantial reduction in engine erosion. However, this impact may vary among the different part of the engine due to the qualitative change in the particle size distribution of the dust as a result of using the filter. A trade off relation is found between erosion reduction and engine power loss due to the use of engine filter.

REFERENCES

1. Fodor, 1979, “Improving Utilization of Potential I. C. Engine Life by Filtration,” Tribology International, 12, pp. 127-129.
2. J. Fodor, 1982, “Improving The Economy of I. C. Engines by Controlling The Contaminations Through Filtration,” World Filtration Congress III, pp. 707-711.
3. El-kotb, M.M., 1988, “Fuels, Oils, and Grease in Cairo Public Transportation,” Academy of science, Research & Technology.
4. El-Sayed, A.F., El-Salmawy, H.A., Shamloul, M.M. and Mesalhy, O.M., 1999, “ Prediction of Erosion Inside the Engine Cylinder Due to Particulated Flow,” SAE paper No. 1999-01-0005, Detroit.
5. G. W. Holmes and R. Overton, 1978, “Experiences with Extended Oil Drain Intervals in Diesel Truck Engines,” SAE Technical Paper 780958, International Fuels & Lubricants Meeting, November 13-16.
6. Jennings, W.H., Head, W.J., and Manning, C.R., 1976, “A Mechanistic Model for the Prediction of Ductile Erosion,” Wear, 40, pp. 93-112.
7. Young, J.P., and Ruff, A.W., 1977, “particle Erosion Measurements of Metals,” J. Eng. Mater. and Tech., 99, pp 121-125.
8. Wai S. Poon and Benjamin Y. H. Liu, 1997, “Fractional Efficiency and Particle Mass Loading Characteristics of Engine Air Filters,” SAE Technical Paper No. 970673.
9. Lefebvre A.H., 1989, “Atomization and Sprays,” Hemisphere Pub. Co..
10. Amsden, A. A., Ramshow, J.D., O’Rourke, P.J. and Butler, T.D., 1989, “KIVA-II: A Computer Program for Chemically Reactive Flows with Sprays,” Loas Alamos National Laboratory Report LA-11560-MS, UC-96.
11. Hamed, A., 1992, ” An investigation in the Variance in Particle Surface Interactions and Their Effects in Gas Turbines,” Journal of Engineering for Gas Turbines and Power, Vol. 114, pp. 235-241.
12. Grant, G., 1973, ”A Model to Predict Erosion in Turbo machinery Due to Solid Particles in Particulate Flow,” Ph.D. Dissertation, Univ. of Cincinnati.

13. Tabakoff, W., and Hamed, A., 1988, “Temperature Effect on Particle Dynamics and Erosion in Radial Inflow Turbine,” ASME, Vol. 110, pp 258-264.